Pupil slicer design for the NASA-NSF extreme precision Doppler spectrograph concept WISDOM

Mark Egan, Gábor Fűrész, Robert Simcoe

MIT Kavli Institute for Astrophysics and Space Research, 77 Massachusetts Ave 37-241, Cambridge, MA 02139

ABSTRACT

The WIYN Spectrograph for Doppler Monitoring (WISDOM) was a concept responding to NASA's solicitation for an extreme precision radial velocity instrument for the 3.5 meter WIYN telescope on Kitt Peak in Arizona. In order to meet the spectral resolution requirement of R = 110,000 while maintaining good throughput and a manageable beam diameter, the front end design of the instrument employed a pupil slicing technique wherein a collimated beam is sliced and fed to six separate fibers. This paper presents the optical and mechanical design of the pupil slicer subassembly, a unique method of dealing with thermally induced defocus error, and the methods and results of aligning a prototype.

Keywords: pupil slicing, exoplanet, spectrograph, PRV, WISDOM, TESS, NASA

1. INTRODUCTION

1.1 WISDOM proposal background

In January 2015, NASA issued an announcement of opportunity to fill the need for a ground-based instrument employing the radial velocity technique to follow up and vet exoplanet candidates discovered by the Kepler space telescope and the soon to be launched Transiting Exoplanet Survey Satellite (TESS). This extreme precision Doppler spectrograph (EPDS) will be integrated on the 3.5 meter WIYN telescope at Kitt Peak in Arizona, with a target of commissioning in 2018. WISDOM was one of two proposals selected for a 6 month funded concept study phase.

1.2 Design context of the pupil slicer

The WISDOM instrument consists of two major assemblies: the front end to be mated to the telescope (see Figure 1), and the spectrograph which is housed in a vacuum chamber in a separate room. These two portions of the instrument are connected by a ~30 meter fiber run. Two identical pupil slicer subassemblies are housed on the front end, taking the collimated beam from an off-axis parabolic mirror and feeding the light into two fiber arms with six fibers each (see Figure 2). A more complete description of the overall instrument and fiber link design can be found in the references.[1,2]
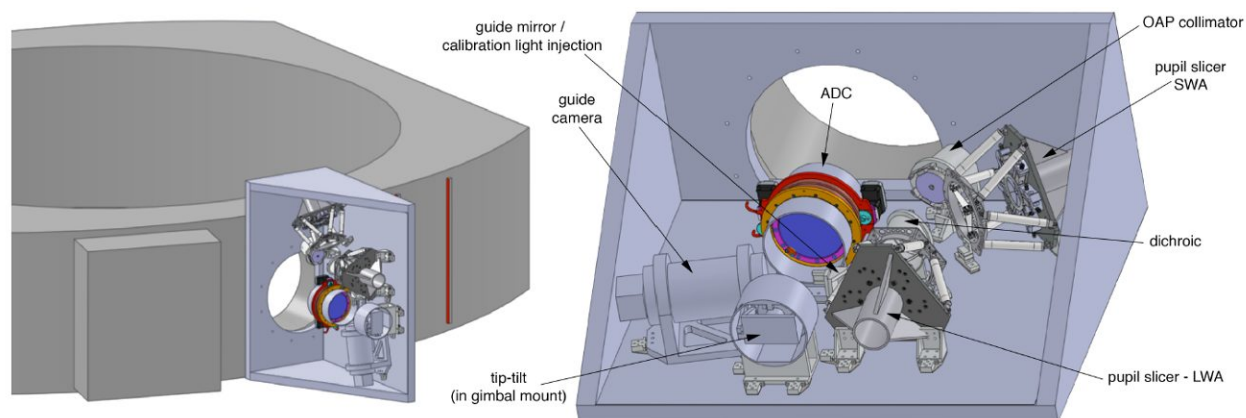

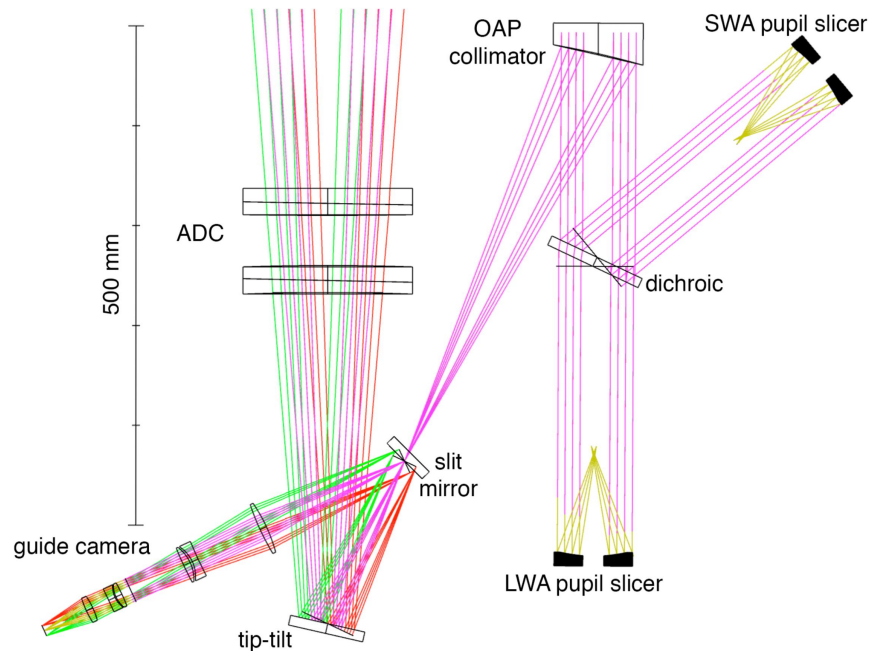Figure 1. WISDOM front end attached to the WIYN telescope mirror cell (left); front end design overview (right).

Figure 2. WISDOM front end optical design overview.

2. OPTICAL DESIGN

2.1 Slicer theory

High spectral resolution is the most important feature of precise Doppler instruments, but diffraction theory dictates that resolving power scales with instrument size, so large instruments have accordingly large complexity and cost. For a telescope of fixed aperture D_{tel} and characteristic slit width ϕ matched to the site seeing, a spectrometer delivers fixed resolution at Littrow:

$$R = \frac{2D_{beam}\tan\delta}{\phi D_{tel}} \tag{1}$$

The value of R flows from scientific requirements, and the blaze angle δ is restricted by grating availability. Hence the collimated beam diameter D_{beam} (which drives instrument size) is essentially specified. For the median site seeing of 0.7″ and a typical echelle blaze of $\tan\delta = 4$, a 170mm diameter beam is needed to meet our requirement of R=110,000 in such a conventional design. For improved throughput it is also desirable to increase the slit width, but for our goal of $\phi = 1.2$ arcseconds the spectrometer would need to be an additional 70% larger if maintaining the R=110k resolution. Project costs scale strongly with beam size and such a design would be difficult to fit within the space constraints of the designated spectrograph room at WIYN.

Fortunately, there is a solution that retains both high spectral resolution and high throughput for a manageable D_{beam}. This technique, called slicing, either subdivides the stellar image at the focal plane (reducing the effective ϕ) or subdivides an intermediate image of the telescope's entrance pupil (reducing the effective D_{tel}) to maintain high R. The slices are remapped into a slit within the spectrograph using optical fibers. While image plane slicing is conceptually simpler, it has the disadvantage that telescope tracking errors and seeing variations change the relative weighting of light between the fibers, and in the simplest configurations the finite thickness of cladding between fiber cores leads to low throughput. WISDOM instead uses a segmented pupil slicer (Figure 3) constructed from a sextet of wedged off-axis paraboloids (OAPs). These are cut out from the same parent mirror, then simply pushed radially towards each other. This effectively closes the gap created by the cutting process and thus forms a segmented but virtually continuous surface that

crosses the converging beams of the segments. This configuration shrinks the plate scale of the telescope and allows the use of a smaller core fiber, thus shrinking the effective size of the spectrograph, reducing cost, and accommodating a much more powerful instrument within the observatory's defined volume envelope.
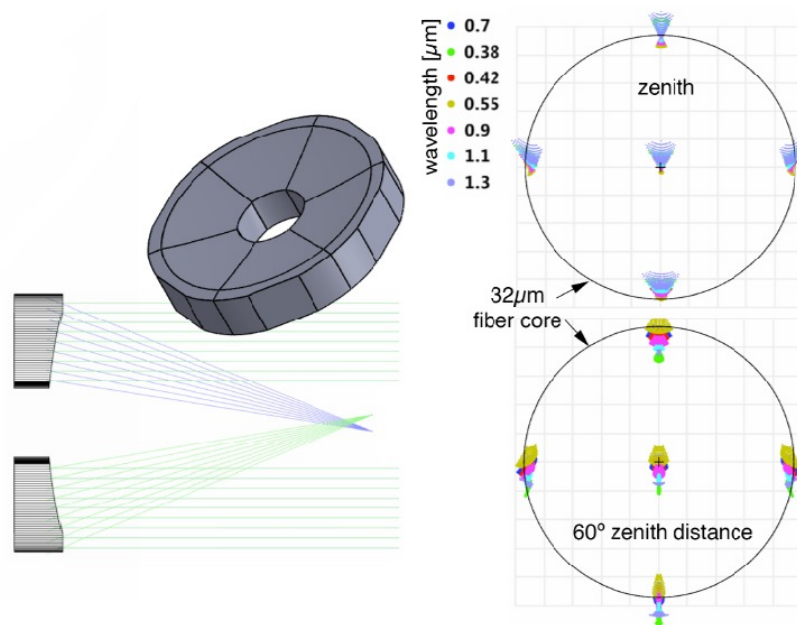

Figure 3. Pupil slicer mirror segment layout (top left), ray trace diagram (bottom left), and image quality via polychromatic spot diagrams for 0, +0.6" field positions overlaid on the 1.2 arcsecond (32μm) fiber core, for air masses of 0 and 2.0. (Spot diagrams are given for the full optical train, including telescope and optics shown in Figure 2).

2.2 WISDOM pupil slicer optical layout and performance

After the primary telescope focus, the diverging F/6 beam is collimated by a single 450mm focal length OAP (see Figure 2). The 75mm parallel beam is split by a dichroic at λ=750nm, defining WISDOM's short- and long wavelength arms. The OAP creates a pupil image 450mm downstream, a conjugate plane to the telescope primary, where the slicer mirrors are located and the light collected by the telescope is fed into 6 fibers. These fibers may be remapped at the output end into a thin but tall pseudo-slit at the spectrograph input. This narrows the slit width (which is proportional to φ) to that of a single optical fiber core, which boosts R without increasing D_{beam}.

The polychromatic image quality (see Figure 3) is excellent at less than 0.1" RMS diameter (compare to 0.7" median seeing FWHM) from zenith all the way down to air mass 2.0, thanks to the use of an all-relective relay/slicer design and a zero-deviation atmospheric dispersion compensator.

3. MECHANICAL DESIGN

3.1 Design overview

The main driver in the design of the pupil slicer assembly is dimensional stability over the -15 / +30 C temperature range experienced at Kitt Peak and the 60 degree gravitational load variation experienced on the WIYN telescope as it tracks targets. Instrument performance requires the stability of the six pupil slicer mirrors with respect to the fiber focal plane to be on the order of approximately 5 microns (0.15 arcseconds, or 1/8 of the fiber diameter) across all environmental variation. Thus materials with extremely low coefficients of thermal expansion (CTE's) that are very rigid are used for the structure of the assembly supporting the slicing mirrors and fibers: Invar36 for the backplate and fiber cone support ring and carbon fiber for the bipod struts connecting these structures. Each Zerodur mirror is bonded to an Invar

mounting tab using Hysol 9313. These mounting tabs are in turn kinematically mounted to the backplate. Shims provide proper mirror – fiber alignment at key interfaces.
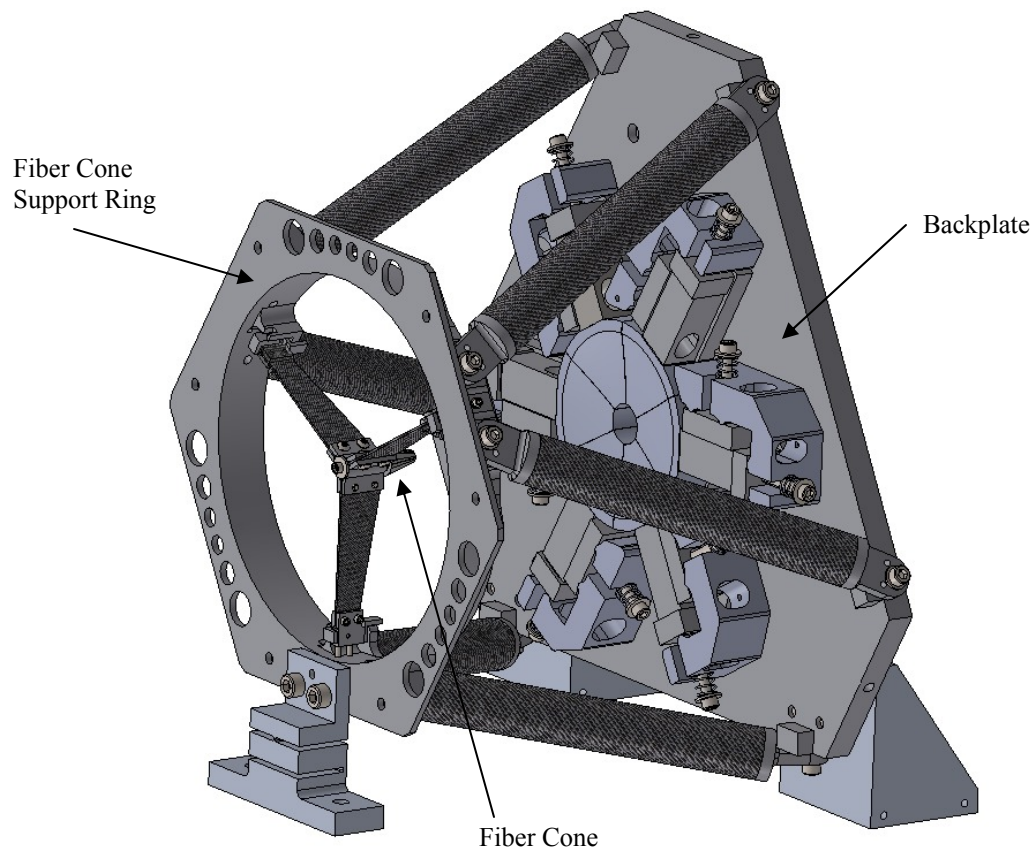
Fiber Cone
Support Ring

Backplate

Fiber Cone

Figure 4. Pupil slicer assembly with the tri-vane mounted fiber cone and kinematically mounted segmented mirrors visible.

3.2 Fiber cone mounting

Each fiber is pointed at the center of a slicer segment, tilted at 13.14° with respect to the optical axis of the slicer, and mounted to a hexagonal cone shown in Figure 5. The cone is made out of fused silica to match the CTE of the fibers and the supporting structure made of Invar and carbon fiber. To secure the fibers, each face of the cone has a V-groove and bonding pockets machined into it by chemically assisted laser etching.
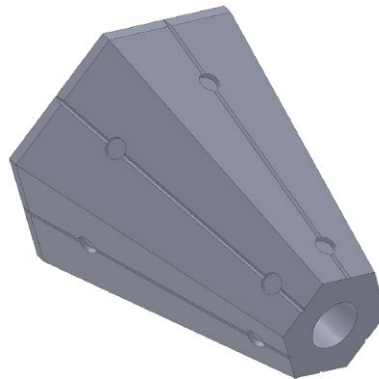
Figure 5. Fused silica fiber cone which houses the six fibers that collect light from the pupil slicer mirrors.

The fiber cone is mounted by three carbon fiber vanes to an Invar support ring as shown in Figure 6. At this interface between the vanes and the support ring shims are used to align the tri-vane subassembly for translation along and rotation about the optical axis, as well as for tip/tilt with respect to the pupil slicer mirror plane. The mirror segments are then adjusted only for lateral alignment.
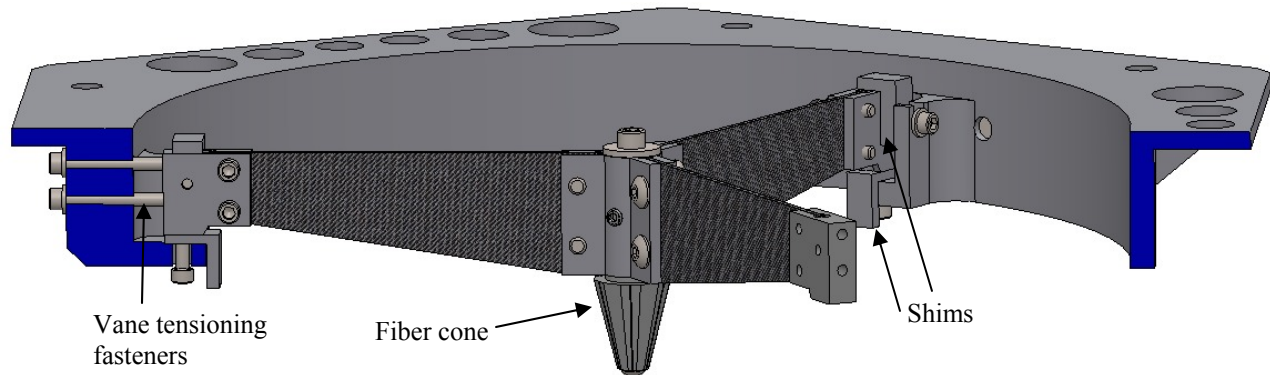

Vane tensioning fasteners

Fiber cone

Shims

Figure 6. Fiber cone subassembly with carbon fiber vanes. Invar support ring is cut away for clear viewing.

3.3 Mirror kinematic mounting

Each mirror segment is bonded to a radially oriented, elongated, rectangular mounting tab (see Figure 7). These mounting tabs are made of Invar to match the CTE of the Zerodur slicer mirror, as well as for dimensional stability over the wide operating temperature range of the front end.

The Invar stems are kinematically mounted and preloaded for 3g against a common Invar backplate structure. The positioning of the segments can be adjusted by lapped Invar shims. During alignment testing, the image locations are determined by optically measuring the foci positions on a flat surface of a fiber dummy cone, with illumination provided by a 100mm collimated beam from a Zygo interferometer. Based on the recorded foci positions on this dummy fiber cone, the proper shim thicknesses for aligning to the fibers are determined, and the shims are adjusted or re-machined. Final alignment can be tweaked by thin plastic shim layers if necessary (see Section 4).
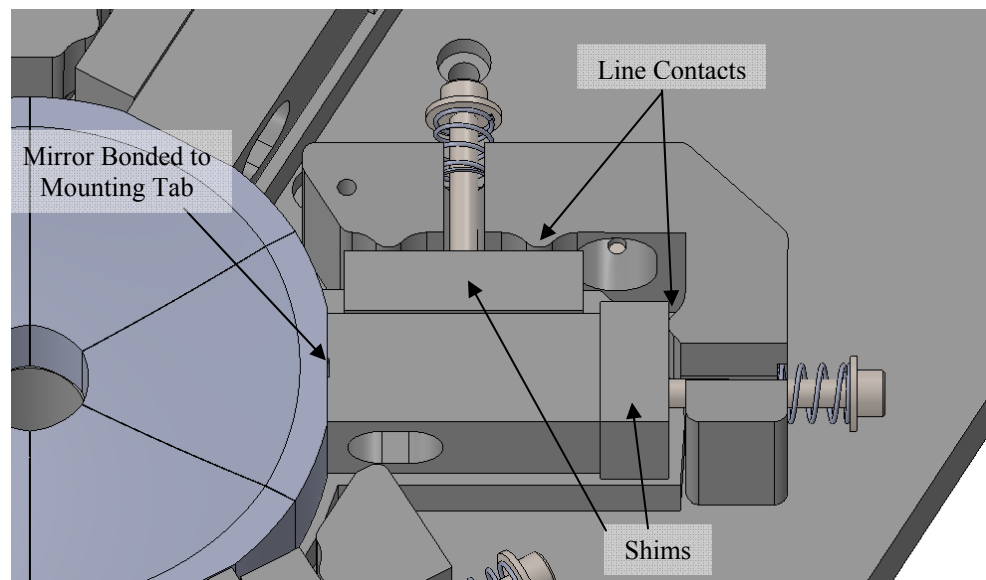

Line Contacts

Mirror Bonded to Mounting Tab

Shims

Figure 7. Mirror segment kinematically mounted. A third fastener and spring set providing preload through the backplate is not visible.

3.4 Mirror bonding to mounting tab

Due to the extreme stability requirements – on the order of several microns over all environmental conditions – the bonding of the pupil slicer mirrors was carefully considered. Because adhesive cannot be bonded in a fashion that is radially symmetric to the optical axis, the bonding material itself must be prevented from causing displacement due to thermal expansion over the -15 / +30 C temperature range. Our approach employed raised contact bosses of 0.25 mm height. The adhesive (blue in Figure 8 below) is applied via syringe through a center hole, seen also in Figure 11.
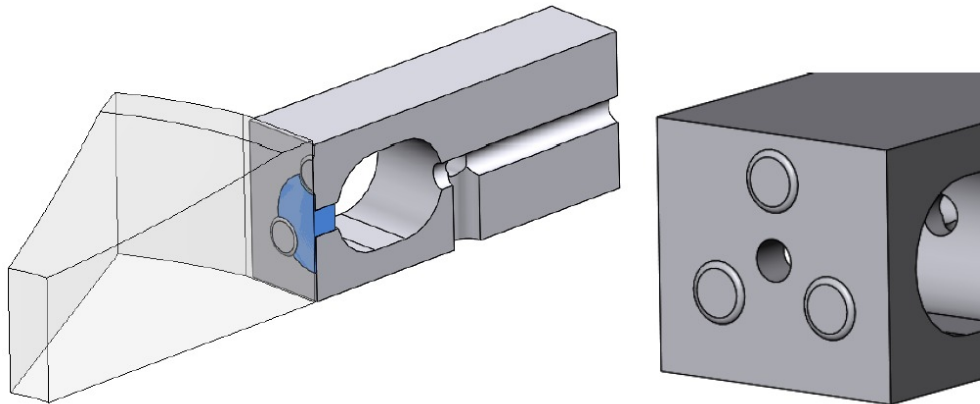

Figure 8. Cross sectional view of a mirror segment and mounting tab with adhesive, the three contact bosses, and the center hole for applying bonding.

As the adhesive contracts in curing, the mirror is preloaded against the contact bosses and the adhesive thickness is then set. The thermal variation induced by the environment then only changes the preload the adhesive provides and doesn't displace the mirror. Hysol 9313 with 40% Siltex 44 fill was used as the adhesive. The contraction ratio of the adhesive must be well known in order to perform FEA analysis of the stress that curing contraction induces into the Zerodur mirror. Our analysis as shown in Figure 9 predicted a maximum Von Mises stress of 3.8 ksi in compression and 1.1 ksi in tension – slightly above the 1 ksi tensile rule of thumb used when bonding optical elements[3] – but low enough to proceed with a prototype.
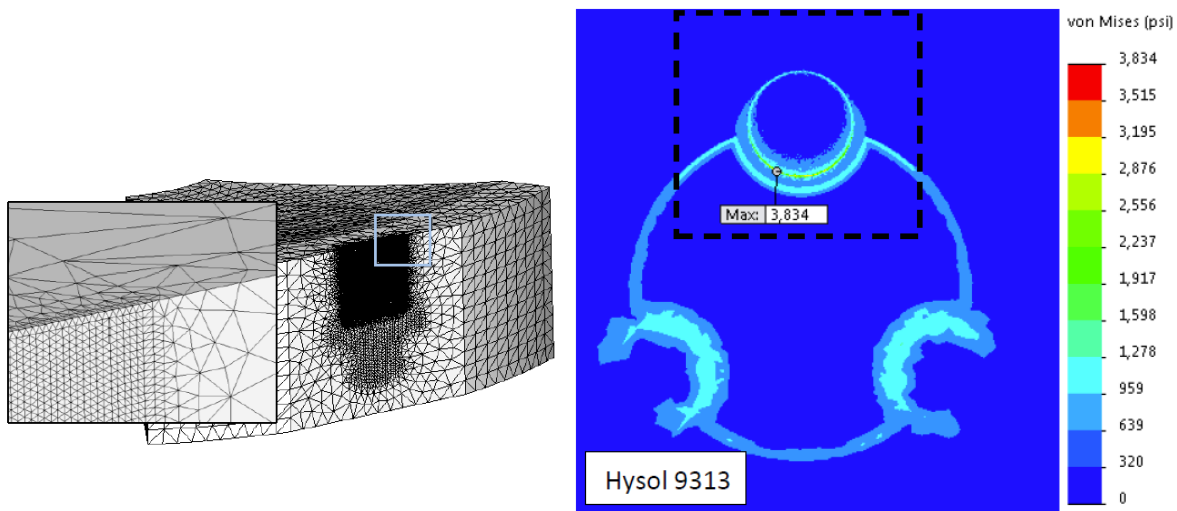

Figure 9. FEA model and analysis results for predicting the adhesive curing stress induced into the Zerodur mirror. Note the high density mesh applied around one of the raised contact pads.

In the process of curing, care must be taken to ensure the mirror and mounting tabs maintain flatness between their bottom surfaces. The fixtures used by our team were built with off-the-shelf Thorlabs components and some custom Delrin pads as shown in Figure 10.
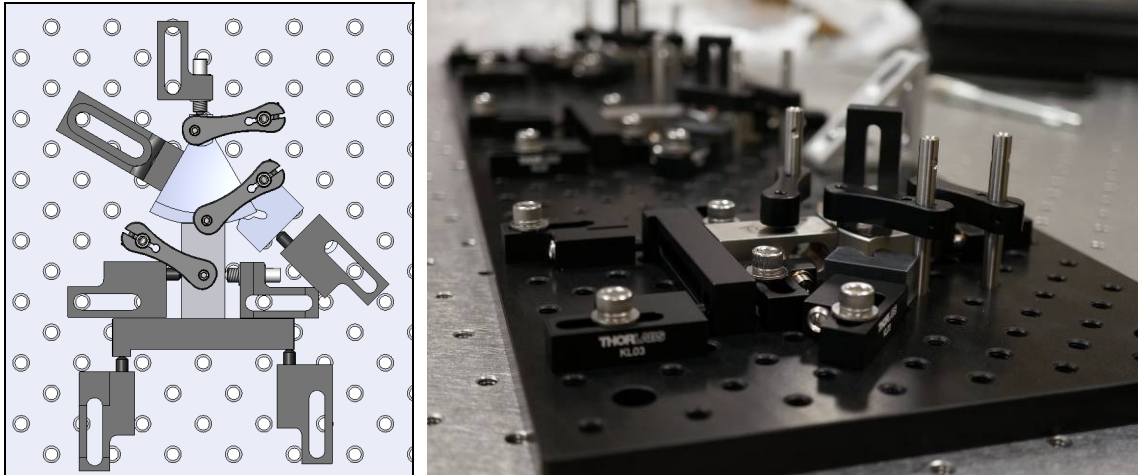

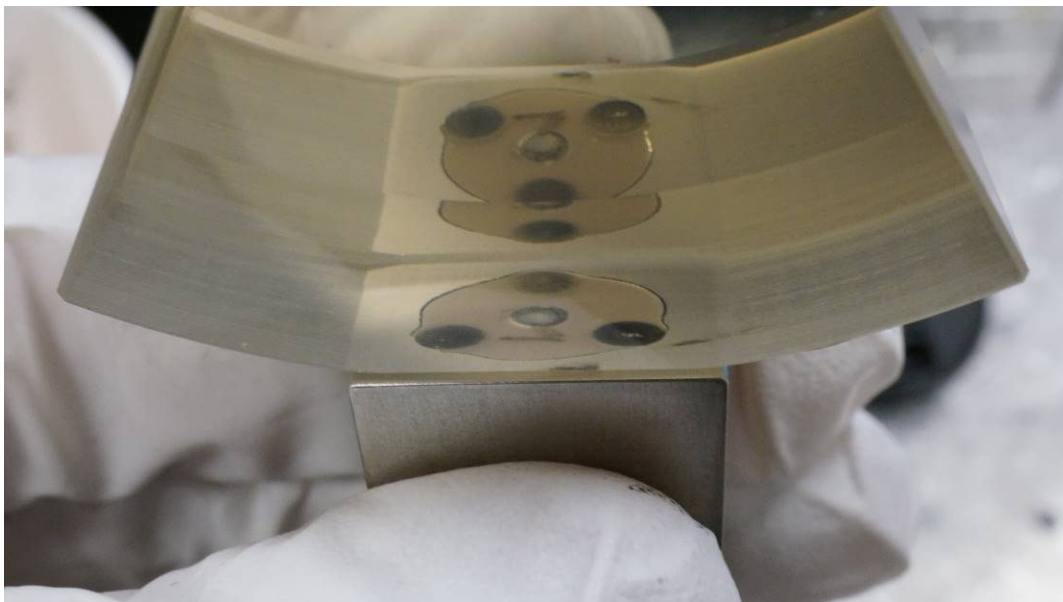Figure 10. Mirror bonding fixtures used for building the pupil slicer prototype.

Figure 11. Mirror bonded to Invar mounting tab using Hysol 9313. The three mounting tab contact bosses and center hole for applying the adhesive with a syringe are clearly visible.

3.5 Offsetting vane thermal deflection

Defocus error occurs when the pupil slicer fiber cone deflects along the collimated beam's optical axis with respect to the pupil slicer mirrors (see Figure 13). The cause of this error is primarily the variation of ambient thermal loading, from -15 to 30 C. Offsetting this error is possible by taking advantage of the thermal expansion and contraction of the fasteners used to tension the vanes shown previously in Figure 6. Since steel fasteners have a higher CTE than the Invar

fiber support ring, under a negative temperature delta the fasteners will contract more than the support ring, increasing fastener preload.

The asymmetric geometry of the vanes combined with different distances between the tensioning fasteners produces a load path that prefers the top of the vain structure, shown in Figure 12 below. This default preload with no temperature delta causes the vanes to deflect the fiber cone in the +Y direction. Under a negative temperature delta, this effect is amplified, producing even more +Y deflection. At the same time, thermal contraction of the carbon fiber struts causes deflection in the opposite (–Y) direction, as shown in Figure 13. For a positive temperature delta the effect is the converse: vane tension relaxes, displacing the fiber cone in the –Y direction while thermal expansion of the struts deflects in the +Y, away from the mirrors. This effect must be fine-tuned by properly configuring the vane geometry, including tensioning fastener location and vane shape, the preload in the top and bottom vane tensioning fasteners, and the associated materials.
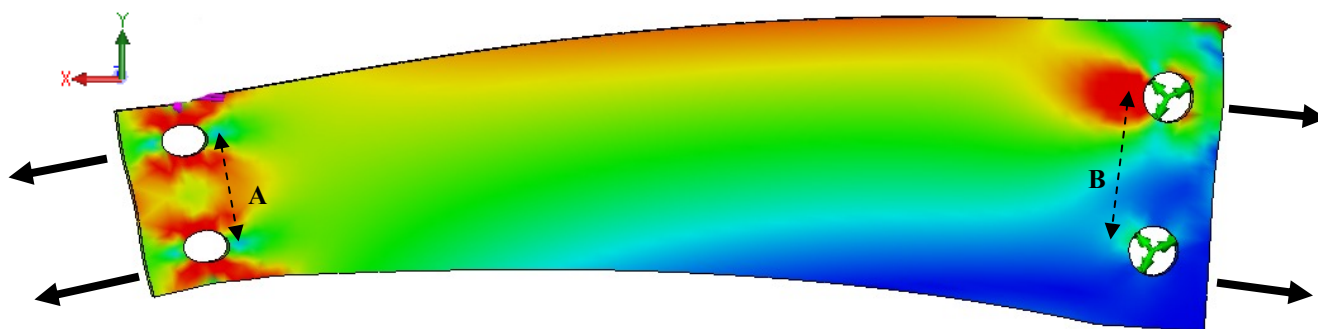

Figure 12. Vane under tension with higher stress shown in red. The trapezoidal shape of the vane with tensioning fastener pairs of different spacing (A & B) results in the fiber cone deflecting in the +Y direction.
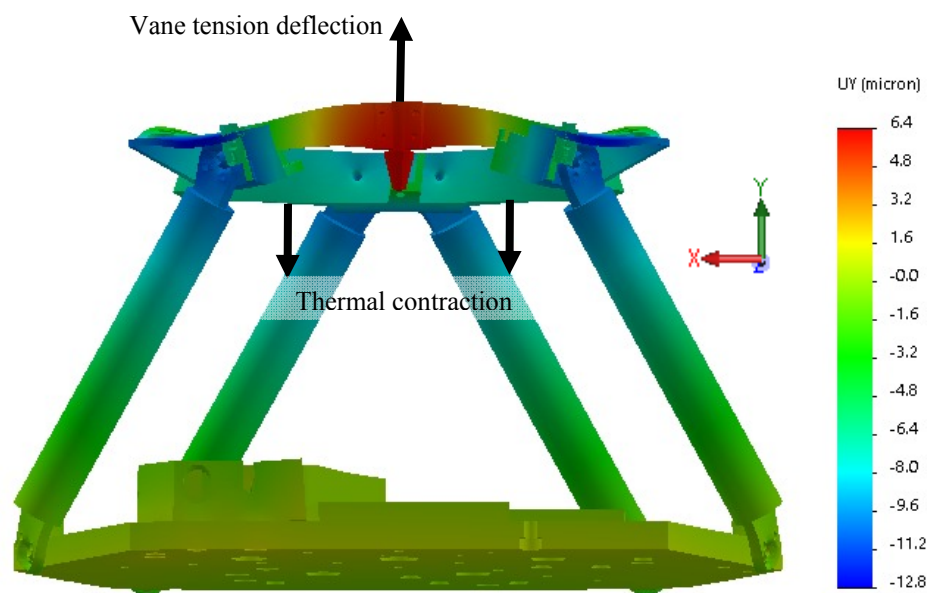

Figure 13. Opposing Y-axis deformations for a negative ΔT: vane and fiber cone deflection in the +Y direction caused by shrinking fasteners and assembly preload, thermal contraction of struts in the –Y direction. Support ring is cut away for better viewing of the fiber cone – vane subassembly.

FEA was used to predict the deflections across several thermal cases. This FEA was performed in SolidWorks. The vane portion of the pupil slicer model uses bonding via rigid links at the trimount-vane interface and two bolt connectors (a

beam element connected to rigid element "wagon wheels" connecting the hole surfaces) at the end mount-fiber support ring interface, shown in blue in Figure 14. Each of these bolts can be configured with a different preload.
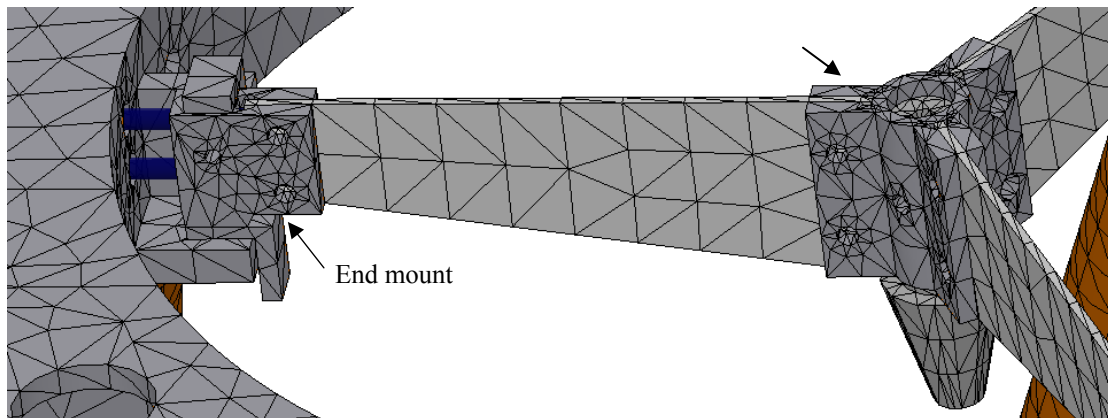

Figure 14. Closeup of vane finite element model

Two different vane geometry configurations were modeled and analyzed: one where the holes on the trimount side were 10mm apart from center to center, and one where they were 6.5mm apart, as shown in Figure 15.
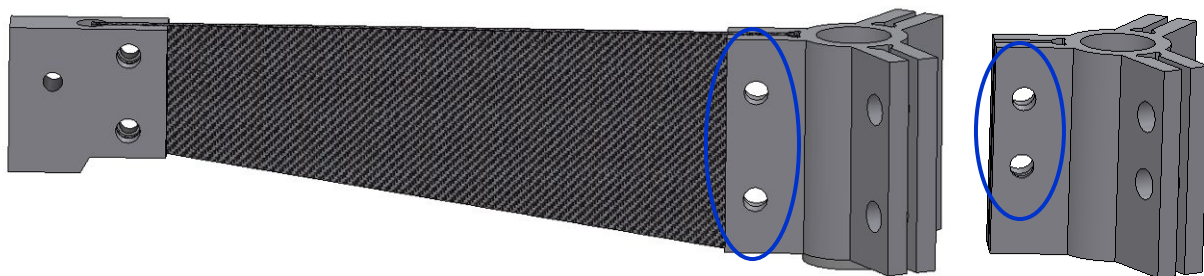

Figure 15. Vane geometries analyzed: 10mm bolt separation at left, 6.5mm at right

Three temperature cases were modeled: -15C, 20C, and 30C, applied as ambient temperature loads. With a zero-stress temperature of 20C (the temperature at which the assembly is integrated), this translates to ΔT's of -35K, 0K and +10K. Sample result plots are shown below in Figure 16 and Figure 17. All results exhibited similar deflections, varying only in magnitude.

A summary of FEA results is shown in Table 1. Predicted Y deflection max-min deltas across the temperature loads were 3.2 microns or less – a vast improvement on the ~15 micron deflection the fiber ring experiences across the temperature ranges.
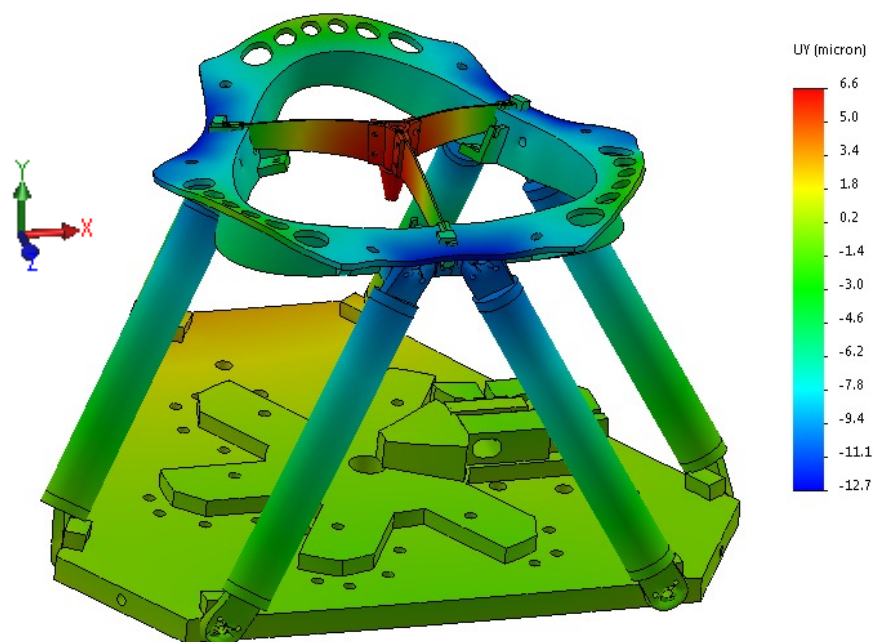
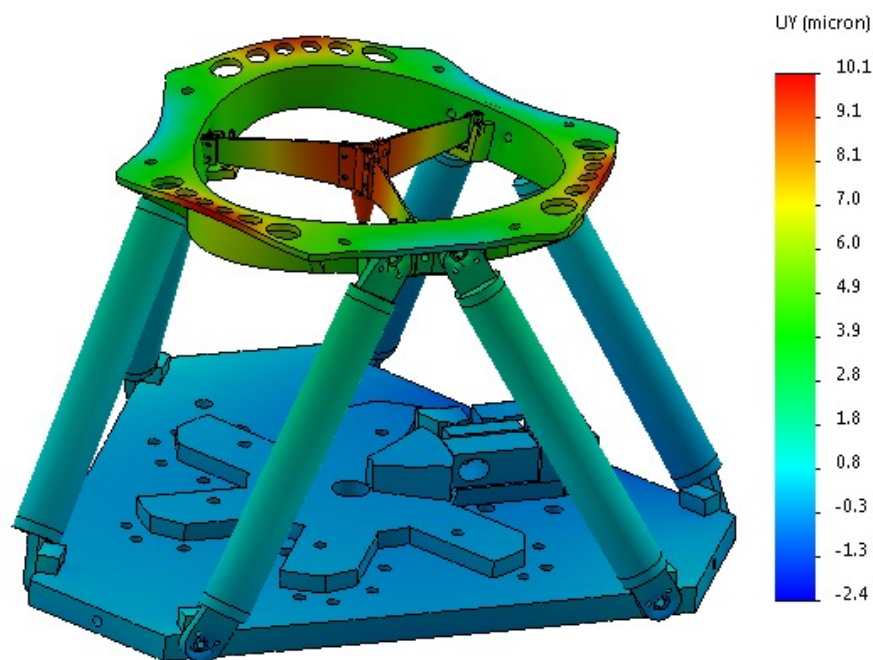Figure 16. Exaggerated Y-Axis deflection of the 10/70, 10mm pupil slicer configuration under a ΔT = -35K thermal load

Figure 17. Exaggerated Y-Axis deflection of the 10/70, 10mm pupil slicer configuration under a ΔT= +10K thermal load

Table 1. FEA Results Summary

Case Description	Vane Tensioning (Top/Bottom, lbf)	Separation Distance of Trimount Bolts (mm)	Y Deflection -35K ΔT (um)	Y Deflection No Temp Load (um)	Y Deflection +10K ΔT (um)	Y Deflection Max-Min Δ (um)
10/70, 10 mm	10/70	10	6.5	7.3	9.7	3.2
10/70, 6.5 mm	10/70	6.5	6.7	5.9	8.1	1.4
70/70, 10 mm	70/70	10	40.3	40.1	42.4	2.3

4. ALIGNMENT

4.1 Alignment method

Once a prototype pupil slicer assembly was built, our team tested the design to ensure that the split beams could be reliably aligned and focused onto the 6 fibers attached to the pupil slicer's fiber cone. Figure 18 shows the basic elements of the setup used to align the pupil slicer: an interferometer producing a collimated beam of light; the pupil slicer assembly located against hard stops; and a camera for monitoring the position and focus of the beams on the fiber plane (looking through the central opening of the slicer mirror that is within the shadow of the telescope secondary mirror on the pupil/slicer mirror plane).
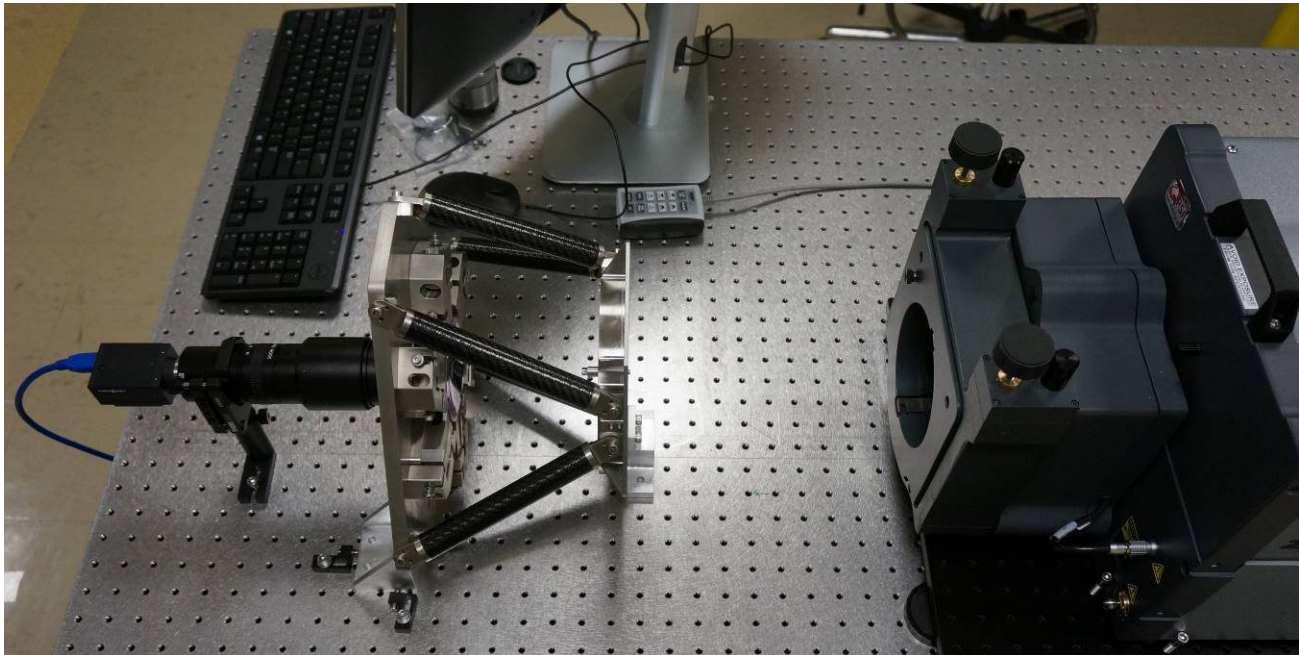

Figure 18. Pupil slicer prototype with interferometer producing a collimated beam on the right and a camera for imaging the fibers through a hole in the pupil slicer backplate on the left.

Figure 19 below shows the six focal points of the sliced beam projected onto a dummy fiber cone prior to alignment and focusing. The camera shown in Figure 18 is used to image the dots with micron-level accuracy in order to determine beam focus and positioning on the fiber cone face where the fiber ends lie.
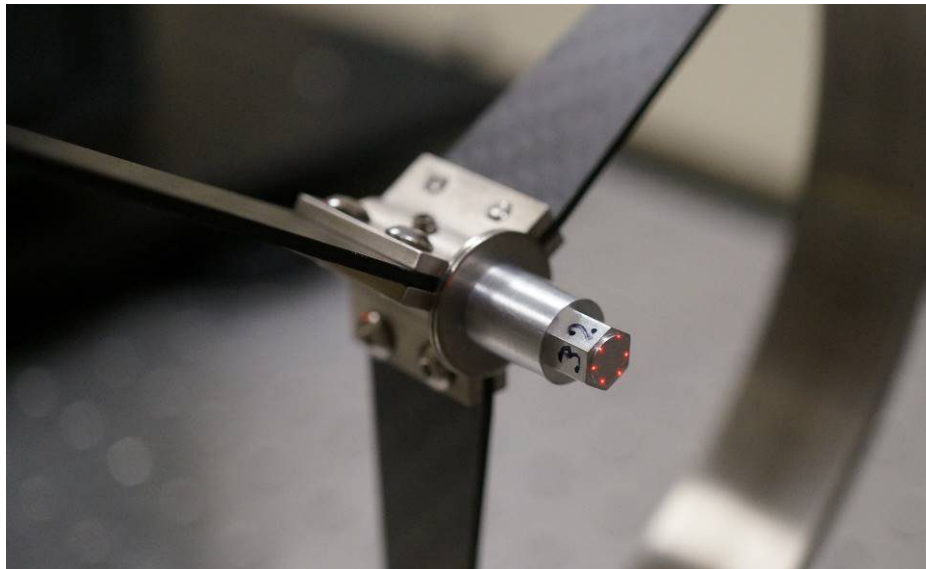
Figure 19. Light from the collimated beam split 6 ways by the pupil slicer and focused onto a dummy fiber cone.

The face of the fiber cone must be very close to parallel with the backplate onto which the mirrors are preloaded. If the fiber cone is tilted, some of the fiber beams will be in focus while others will not. The focus of the 6 beams can be adjusted in two ways: first by increasing shim thicknesses shown previously in Figure 6, and secondarily by increasing preload on the fasteners tensioning the individual vanes to produce the required vane deflections.

Once the beams are all in focus, their positions on the face of the fiber cone can be adjusted by modifying the thickness of the shims that locate the mirrors via their mounting tabs as shown previously in Figure 7. For the operational instrument, the Invar shims would be machined with micron precision via lapping operations to change their thickness. In the lab, plastic shims of varying thickness were used to verify the concept, shown below in Figure 20.
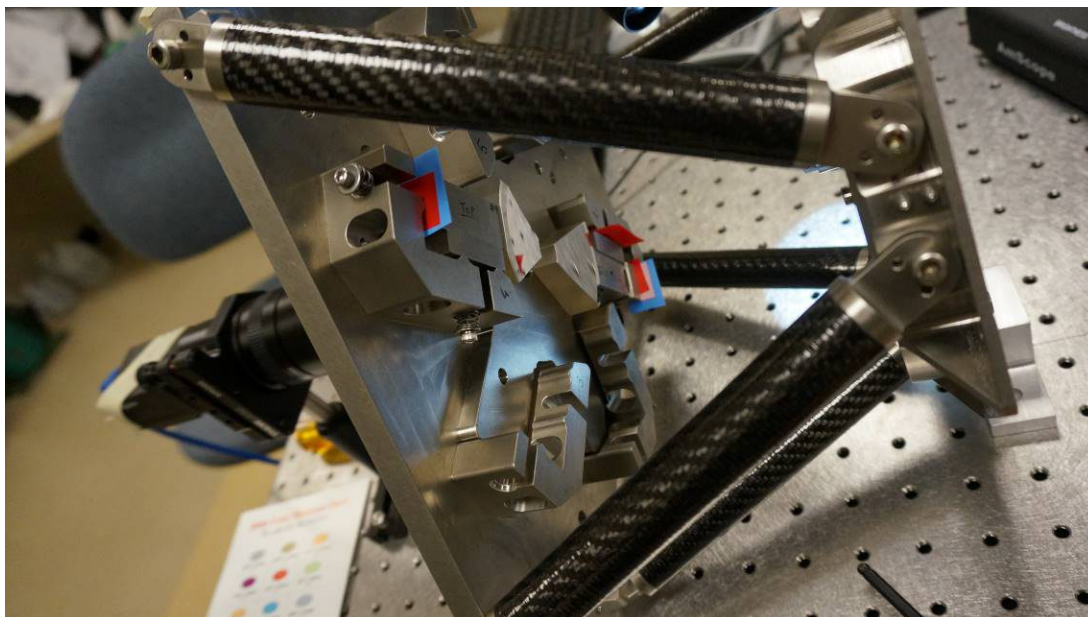

Figure 20. Aligned mirrors with plastic shims of varying thicknesses visible.

Two mirrors were focused and aligned to two fibers bonded to the prototype dummy cone. Two mirrors are the minimum number needed to verify the concept. A single focused and aligned beam cannot verify that the fiber cone is

parallel to the mirror mounting plane. Although three beams are necessary to fully constrain the parallelism of the plane, two are sufficient to prove the ability to adjust tip and tilt with precision and repeatability.

4.2 Results

Figure 21 below shows the camera output for two focused beams prior to alignment to the fibers. White light was fed into the opposite ends of the fibers in order to make them visible to the camera – at 32 microns in core diameter they would otherwise not be visible.
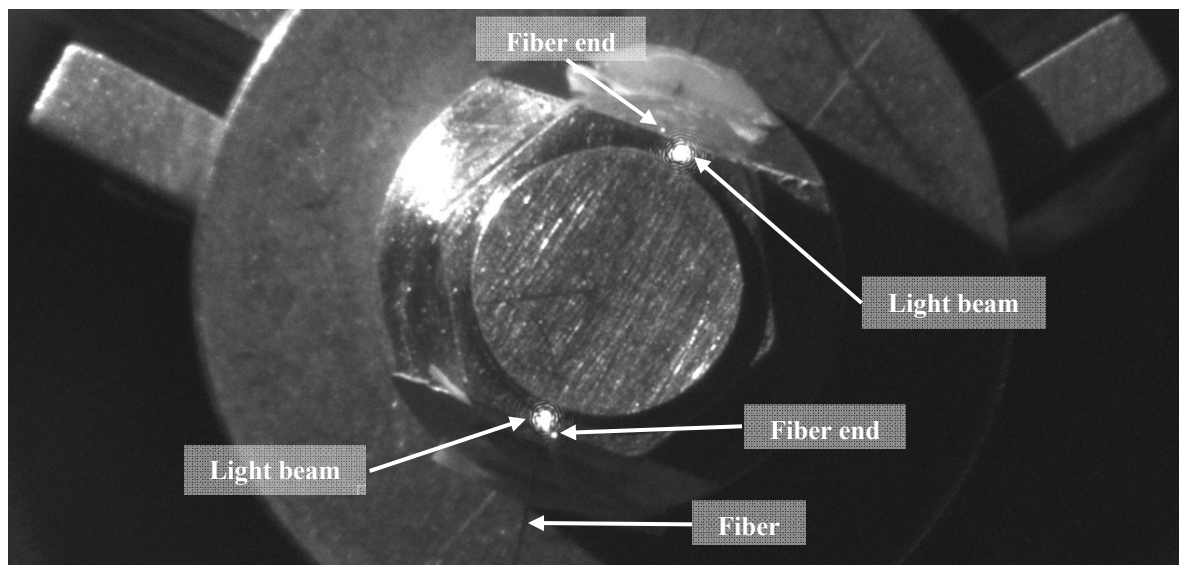

Figure 21. Image of two focused beams of light on the dummy fiber cone, prior to alignment with the fibers. The fibers are bonded to this cone, and are clearly visible because they are back-illuminated with an LED light (at their opposite ends, outside of the picture).

Figure 22 shows images similar to Figure 21, but with shorter exposure times, so that the true size of the beams can be seen. In the image at left the alignment of the beams is much closer, though not perfect. In the image at right, full alignment of both beams to the fibers has been achieved.
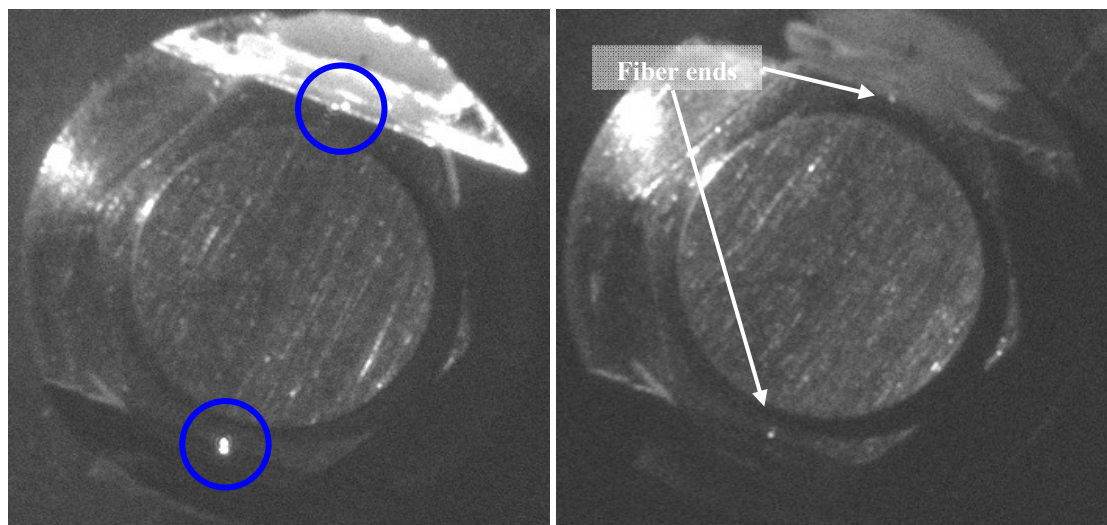

Figure 22. Partial alignment of the beams to the fibers at left; full alignment at right.

Precision alignment of the mirrors and fiber cone can be achieved by maximizing the light intensity emerging from the fiber ends, as shown in Figure 23.
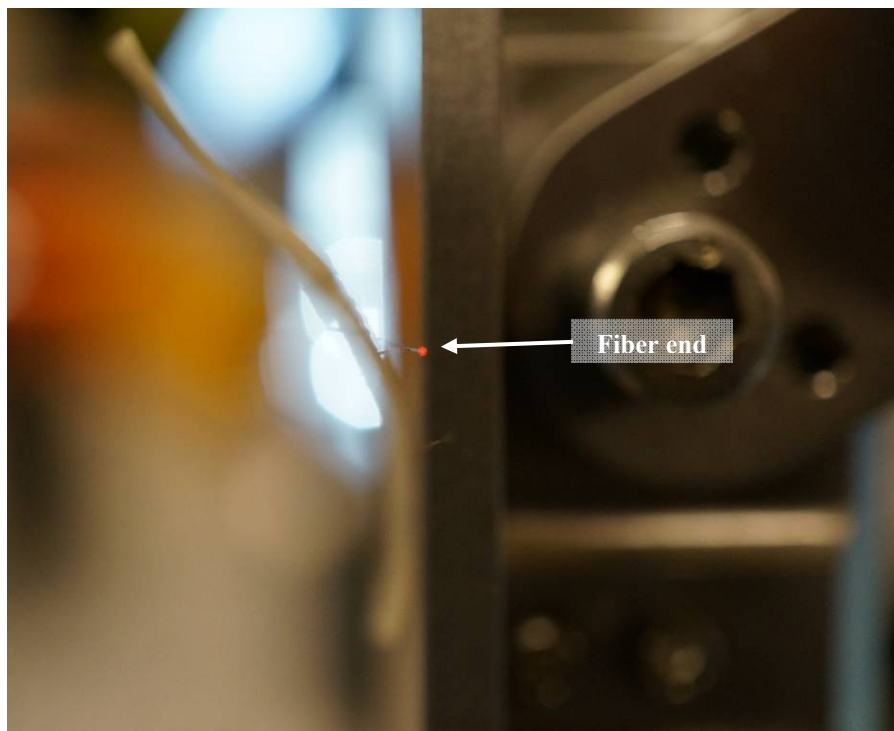

Figure 23. Fiber end showing collected light from the pupil slicer assembly and interferometer.

5. CONCLUSION

WISDOM, a precision radial velocity instrument proposed for the WIYN telescope at Kitt Peak, employs a unique pupil slicer in its front end design. This all-reflective pupil slicer delivers exceptional image quality and high throughput, while dissecting the beam into six segments that are then individually focused on fibers mounted to a vane structure using a series of shims and fastener preload adjustments. This vane structure design attempts to passively counteract thermal defocusing effects due to large temperature swings seen at Kitt Peak.

Our team has built a prototype of this pupil slicer and demonstrated the ability to focus and align the beams onto the fibers. The design ensures, as shown by FEA analysis, the stability of the alignment over variations in thermal and gravity loads due to pointing of the telescope. We also verified the design of the vane thermal offset feature, which analysis shows to reduce thermal deflection of the fiber cone from 15 microns to 3 over the +20/-15C temperature range seen at Kitt Peak.

REFERENCES

[1] Fűrész, G., et al. "WISDOM: the WIYN spectrograph for Doppler monitoring: a NASA-NSF concept for an extreme precision radial velocity instrument in support of TESS," Proc. SPIE 9908-41 (2016).
[2] Fűrész, G., et al. "Fiber link design for the NASA-NSF extreme precision Doppler spectrograph concept WISDOM", Proc. SPIE 9908-281 (2016).
[3] Yoder, P., Vukobratovich, D. [Opto-Mechanical Systems Design], CRC Press, Boca Raton, p.387, 2006.
[4] Bouchy, F., Pepe, F., Queloz, D., "Fundamental photon noise limit to radial velocity measurements," Astronomy and Astrophysics v.374, p.733-739 (2001).